Chapter 6

Non-local detection of resistance fluctuations of an open quantum dot

Abstract

We investigate quantum fluctuations in the non-local resistance of an open quantum dot which is connected to four reservoirs via quantum point contacts. In this four-terminal quantum dot the voltage path can be separated from the current path. We measured non-local resistance fluctuations of several hundreds of Ohms, which have been characterized as a function of bias voltage, gate voltage and perpendicular magnetic field. The amplitude of the resistance fluctuations is strongly reduced when the coupling between the voltage probes and the dot is enhanced. Along with experimental results, we present a theoretical analysis based on the Landauer-Büttiker formalism. While this theory predicts non-local resistance fluctuations of about 20 times larger amplitude than what has been observed, agreement with theory is very good if it is scaled with a factor that accounts for the influence of orbital dephasing inside the dot. This latter case is in reasonable agreement with an independently determined time scale for orbital dephasing in the dot.

This chapter is based on Ref. 8 on p. 131.

6.1 Introduction

When a conducting solid-state system is smaller than the phase coherence length of the electrons, its electrical conductance is significantly influenced by quantum interference. For diffusive thin films this results in phenomena known as universal conductance fluctuations and weak localization [1, 2, 3, 4]. Similar conductance fluctuations and localization phenomena are observed in micron-scale ballistic quantum dots, since these behave in practice as chaotic cavities due to small shape irregularities in the potential that defines the dot. These conductance fluctuations have been extensively studied for two-terminal quantum dots [5, 6, 7, 8], *i.e.* systems with only a source and a drain contact. However, for quantum dots this two-terminal conductance is often influenced by Coulomb blockade and weak localization effects, which complicate an analysis when one aims at studying other effects.

We present here a study of fluctuations in electron transport in a *four*-terminal ballistic quantum dot. The dot is coupled to four reservoirs via quantum point contacts (QPC). In such a system, the voltage path (with probes at voltage V_+ and V_-) can be separated from the path that is used for applying a bias current I (see Fig. 6.1). Consequently, one can measure so-called *non-local* [9, 10, 11, 12] voltage signals that are purely due to quantum fluctuations of the chemical potential [13] inside the dot, and for which a naive classical analysis predicts a signal very close to zero. For linear response, this is expressed as a non-local resistance $R_{nl} = (V_+ - V_-)/I$ (this non-local resistance will fluctuate around a value that is very close to zero Ohm, and is therefore studied in terms of resistance rather than conductance). Increasing the number of open channels in the voltage probes will result in enhanced dephasing for the electronic interference effects. With a four-terminal system, one can study this directly since it results in a reduction of the amplitude of the non-local resistance fluctuations. Notably, such a reduction of the fluctuation amplitude does not occur upon increasing the number of open channels in a two-terminal system [14]. Furthermore, such a four-terminal systems could be used for studying signals that are due to spin. In a strong magnetic field QPCs can be operated as spin-selective injectors or voltage probes [15]. This can be used to generate and detect an imbalance in the chemical potential for spin-up and spin-down electrons [16], similar to non-local spin-valve effects observed in metallic nanodevices [17]. Also here, a four-terminal dot is an interesting alternative to work on spin physics in dots with two-terminal devices [18, 19, 20]. However, if such a system is smaller than the electron phase

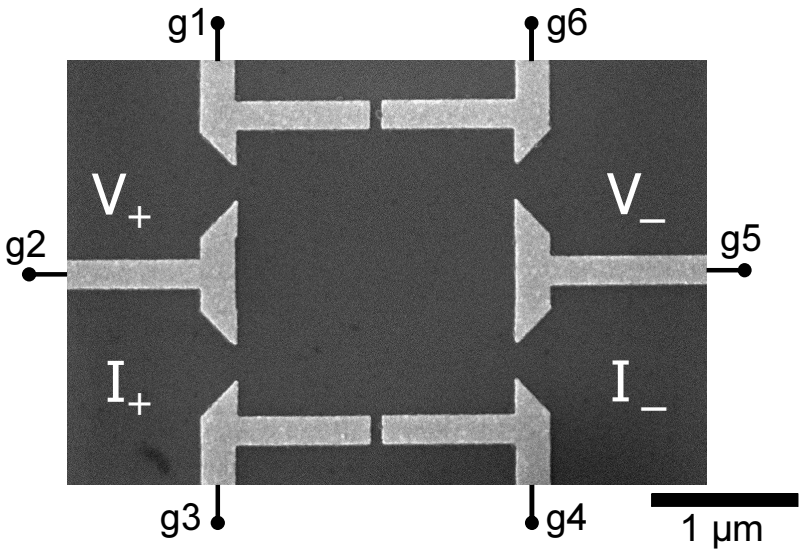

Figure 6.1: Electron microscope image of the device studied in this article. The position of the reservoirs used for current biasing (I_+ and I_-) and voltage probes (V_+ and V_-) is indicated, as well as the numbering of the gates labeled $g1$-$g6$. Unless stated otherwise, all results presented in this article were obtained in this non-local configuration.

coherence length, the non-local signals with information about spin will also show fluctuations that result from interference of electron trajectories [21].

In this chapter, we focus on our first experiments with such a four-terminal quantum dot. We aimed at characterizing the non-local resistance fluctuations, and studying the influence of the voltage probes on the typical amplitude of these fluctuations. As a comparison with our experimental results we present a numerical simulation of the non-local resistance, based on the Landauer-Büttiker formalism [9, 22] and the kicked rotator [23, 24].

The outline of the chapter is as follows: Section 6.2 presents the experimental realization. In section 6.3, we present measurements of the non-local resistance as a function of bias voltage, gate voltage, and magnetic field, and confirm that the observed fluctuations in the non-local resistance are the four-terminal equivalent of universal conductance fluctuations in two-terminal systems. In section 6.4, we analyze how the typical amplitude of the measured non-local resistance fluctuations depends on the number of open channels in the voltage probes. Section 6.5 presents our theoretical analysis with a comparison to the experimental results, before ending with conclusions.

6.2 Experimental realization

Our device was fabricated using a GaAs/$Al_xGa_{1-x}As$ heterostructure containing a two dimensional electron gas (2DEG) 75 nm below the surface, purchased from Sumitomo Electric Co. At 4.2 K, the mobility was $\mu = 86$ m^2/Vs and the electron density was $n_s = 2.4 \cdot 10^{15}$ m^{-2}. The dot was designed with an area of 2×2 μm^2. Figure 6.1 shows and electron microscope image of the device. Six depletion gates were deposited on the surface (15 nm of Au with a Ti sticking layer) and were used for defining the dot in the 2DEG. We estimate that the depletion width around the gates was about 100 nm, such that the electron gas area A_{dot} inside the dot was about 3.2 μm^2. With these six gates the dot could be coupled to the four reservoirs via QPCs in a controllable manner. All four QPCs showed clear quantized conductance steps [25, 26] in measurements where only the corresponding pair of gates were depleting the 2DEG. Note that throughout this article we use that a QPC with a conductance of $2e^2/h$ is defined as having one open channel (denoted as $N = 1$), *i.e.* we neglect spin when counting channels. The four reservoirs were connected to macroscopic leads via Ohmic contacts, which were realized by annealing a thin Au/Ge/Ni layer that was deposited on the surface.

All the measurements were performed with the sample at a temperature of 130 mK. However, the temperature dependence of our data saturated when cooling below $\approx$ 400 mK, so we will assume this value for the effective electron temperature. We used a current bias I with standard ac lock-in techniques at 13 Hz. Unless stated otherwise, we used $I = 1$ nA. The non-local resistance R_{nl} was then recorded as the zero-bias differential resistance dV/dI, with V defined as $V \equiv V_+ - V_-$. We used a floating voltmeter to measure V, thus being insensitive to the voltage across the dot along the current path, and thereby insensitive to Coulomb blockade and weak localization effects. On the current path, only the I_- reservoir was connected to the grounded shielding of our setup, and all gate voltages were applied with respect to this ground.

A magnetic field could be applied, with an angle of 7° with respect to the 2DEG plane (determined from standard Hall measurements and electron focusing effects, discussed below). The perpendicular component of this field was used for studying the dependence of the non-local resistance on perpendicular magnetic field. The component of the magnetic field parallel with the 2DEG plane was oriented perpendicular to the current path. While this parallel field was about ten times stronger than the perpendicular field, the orbital effects associated

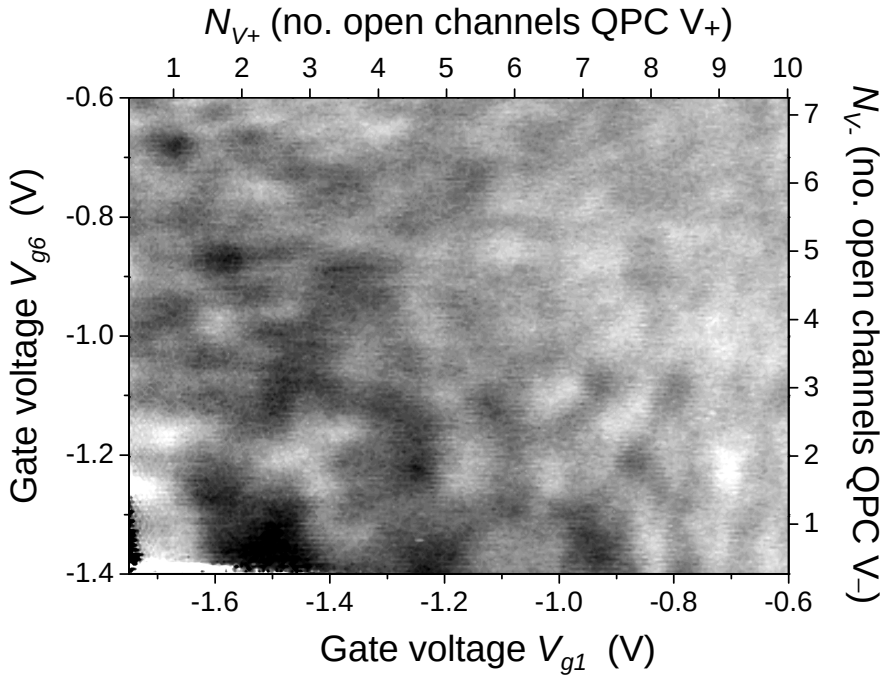

Figure 6.2: Gray scale plot of the non-local resistance R_{nl} as a function the voltages applied to gates $g1$ and $g6$. The axes also show the corresponding number of open channels for the V_+ and V_- probes. The gray scale shows R_{nl} at a scale from $-500\ \Omega$ (black) to $500\ \Omega$ (white). The value of R_{nl} fluctuates around zero Ohm, with a typical amplitude that decreases when the number of open channels in the V_+ and V_- probes increases. The QPCs formed by gates $g2$ and $g3$, as well as $g4$ and $g5$ (defining the current path) had a fixed conductance of $2e^2/h$ each. Data taken in zero magnetic field at 130 mK.

with this parallel field are negligibly small, and it can be disregarded for all of the experimental results presented here (and weak enough to not significantly reduce the amplitude of resistance fluctuations [27, 28, 29]).

6.3 Non-local resistance fluctuations

Figure 6.2 shows the non-local resistance R_{nl} as a function of the voltage applied to gate $g1$ and gate $g6$. The other four gate voltages were kept constant during this measurement, with the QPCs in the current path at a conductance of $2e^2/h$ each (one open channel, $N = 1$). The range of gate voltage for $g1$ and $g6$ used here corresponds to opening the voltage-probe QPCs from nearly pinched off ($N = 0$) up to about $N = 8$ open channels. As a function of these gate voltages,

the non-local resistance shows a random pattern of fluctuations around zero Ohm, with maximums and minimums up to about $\pm 500\ \Omega$. Notably, the change in gate voltage needed to change R_{nl} significantly (one fluctuation), is very similar to the change in gate voltage needed for increasing the number of open channels in a QPC by one. This corresponds to changing the shape of the potential that forms the dot by a distance of about half a Fermi wavelength, which is consistent with the length scale needed for significantly changing a random interference pattern of electron trajectories. These non-local resistance fluctuations as a function of the gate voltage on $g1$ and $g6$ were highly reproducible, and indeed a so-called finger print of the sample. The identical measurement repeated after 4 days (during which we performed strong magnetic field sweeps and a temperature cycle up to 4.2 K) showed nominally the same fluctuation pattern as in Fig. 6.2.

In Fig. 6.3 we present results of studying the dependence of the amplitude of the non-local resistance fluctuations on the amplitude of the applied bias current I. The figure shows measurements of R_{nl} as a function of the gate voltage V_{g1}. The results show several fluctuations that are reproducible, but decreasing in amplitude upon increasing the amplitude of the bias current. In this experiment, the conductance of the other three QPCs was fixed at $2e^2/h$. The amplitude of the fluctuations reduces when the measurement averages over contributions of electrons in uncorrelated orbitals, that is, averaging over electrons that differ in energy by more than the Thouless energy [3, 4]. When the current bias is increased, the corresponding voltage bias V_{bias} increases as well (see labels in the Fig. 6.3), and this is used to experimentally estimate the Thouless energy E_{Th} for our system. The amplitude of the fluctuations starts to decrease significantly around $V_{bias} \approx 125\ \mu$V. This is close to a theoretical estimate [30, 31] for $E_{Th} = \frac{\hbar v_F}{L} \approx 80\ \mu$eV, where v_F the Fermi velocity and L the effective width of the dot.

We now turn to measurements of the non-local resistance as a function of perpendicular magnetic field, presented in Fig. 6.4a. Here the conductance of all four QPCs was fixed at $2e^2/h$. The trace of R_{nl} shows random fluctuations of similar amplitude as observed in the gate voltage dependence. For estimating the typical magnetic field scale that significantly changes the value of R_{nl} (the correlation field ΔB_c), we apply an established method from such studies on similar two-terminal quantum dot systems (following Refs. [32, 33]). For this, we took the averaged power spectrum $S_B(f_B)$ of traces as in Fig. 6.4a (only using the low-field data in the range ± 140 mT, see below). On a logarithmic scale, $S_B(f_B)$ closely resembles a straight line with negative slope in the frequency range between $f_B = 0.05$ and 0.5 cycles per mT (and then levels off),

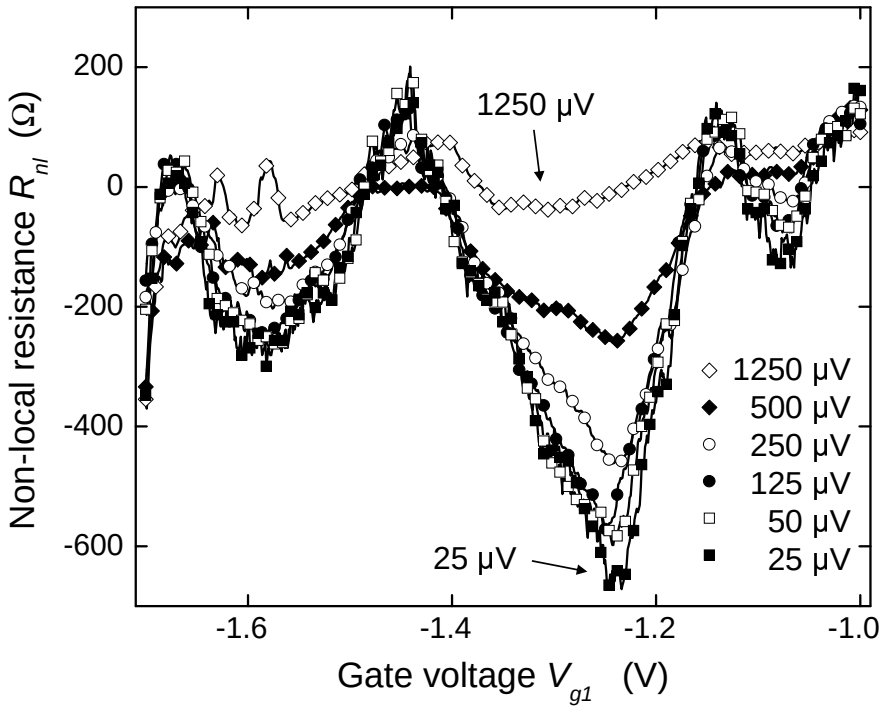

Figure 6.3: The non-local resistance R_{nl} as a function of the voltage V_{g1} applied to gate $g1$, taken for different amplitudes of the bias current I in the lock-in detection scheme (from 1 nA up to 50 nA). The legend shows the corresponding values for the voltage drop across the quantum dot along the current path, obtained as $V_{bias} \approx I \times \frac{2}{2e^2/h}$. The curves show a reduction of the amplitude of the non-local resistance fluctuations with increasing V_{bias}. The conductance of the QPC formed by $g5$ and $g6$ (defining the V_- probe) is set at $2e^2/h$. For further experimental parameters see Fig. 6.2.

very similar to the results from the studies with two-terminal dots [32, 33]. We fit this part of the spectrum to the form predicted by semiclassical theory [32, 33], $S_B(f_B) = S_B(0)(1 + 2\pi\alpha\phi_0 f_B) \cdot \exp(-2\pi\alpha\phi_0 f_B)$, where $\phi_0 = h/e$ the flux quantum, and α the inverse of an effective area for orbitals in the dot which defines $\Delta B_c = \alpha\phi_0$. This yields $\Delta B_c = 2.1 \pm 0.8$mT (the large error bar must be assumed since we could only measure a small number of independent fluctuations for this analysis). This is in good agreement with theory for universal conductance fluctuations [3], which predicts $\Delta B_c \approx \frac{\phi_0}{A_{dot}} = 1.3$ mT (simply expressing the magnetic field needed for adding one flux quantum ϕ_0 through the area of the dot). It is commonly observed that ΔB_c is enhanced by a factor up to about ~ 2 due to flux cancelation effects for electrons that move ballistically between

the edges of the dot [34, 2, 30]. The measured value for ΔB_c is also in agreement with the observation of a weak-localization peak around zero magnetic field [3] observed in the two-terminal resistance (breaking the time-reversal symmetry), which has a width of the same order of magnitude as ΔB_c.

For confirming that changing the field by more than ΔB_c gives access to a statistically independent set of fluctuations, we studied fluctuations in R_{nl} as a function of gate voltage V_{g1}, for different values of the perpendicular field (Fig. 6.4b). This data confirms that changing the perpendicular magnetic field in steps of 14 mT gives access to completely different patterns of random fluctuations in R_{nl}.

The inset of Fig. 6.4a shows the appearance of much higher peaks in R_{nl} (up to 3 kΩ) for perpendicular magnetic fields stronger than $\pm$140 mT. We could confirm that these peaks are due to electron focusing and skipping orbit effects. With only the three gates $g1$, $g2$ and $g3$ depleting the 2DEG, our device is identical to devices used for electron focusing experiments by Van Houten *et al.* [35], and we observe very similar focusing peaks as in this work at only one polarity of the magnetic field. With the dot formed, these effects cause peaks in R_{nl} at both polarities of the magnetic field. The onset of these effects at $\pm$140 mT agrees with a focusing radius of about 1 μm.

6.4 Influence of voltage probes

The presence of additional voltage probes on a quantum dot system will act as source of dephasing for the electrons in the dot, and this effect should increase when the coupling between the dot and the probe reservoirs is enhanced. Earlier work recognized that non-local voltage probes on a mesoscopic system are a source of dephasing [36, 37], and in theoretical work an additional voltage probe is often used to model a source of dephasing [38, 39]. This can be directly studied with our system. The amplitude of the non-local resistance fluctuations (which result from electron phase coherence) should decrease when the voltage probes are tuned to carry more open channels. To study this effect we used data sets of the type presented in Fig. 6.2. We concentrate on the case where the time-reversal symmetry is broken ($\beta = 2$) by applying weak magnetic fields, since this allows us to get statistics from a larger set of data.

For a data set as in Fig. 6.2, the total number of open channels in the voltage probes ($N_{V+} + N_{V-}$) is lowest in the bottom left corner of the graph, and highest in the top right corner. Inspection of R_{nl} in Fig. 6.2 confirms that the typical

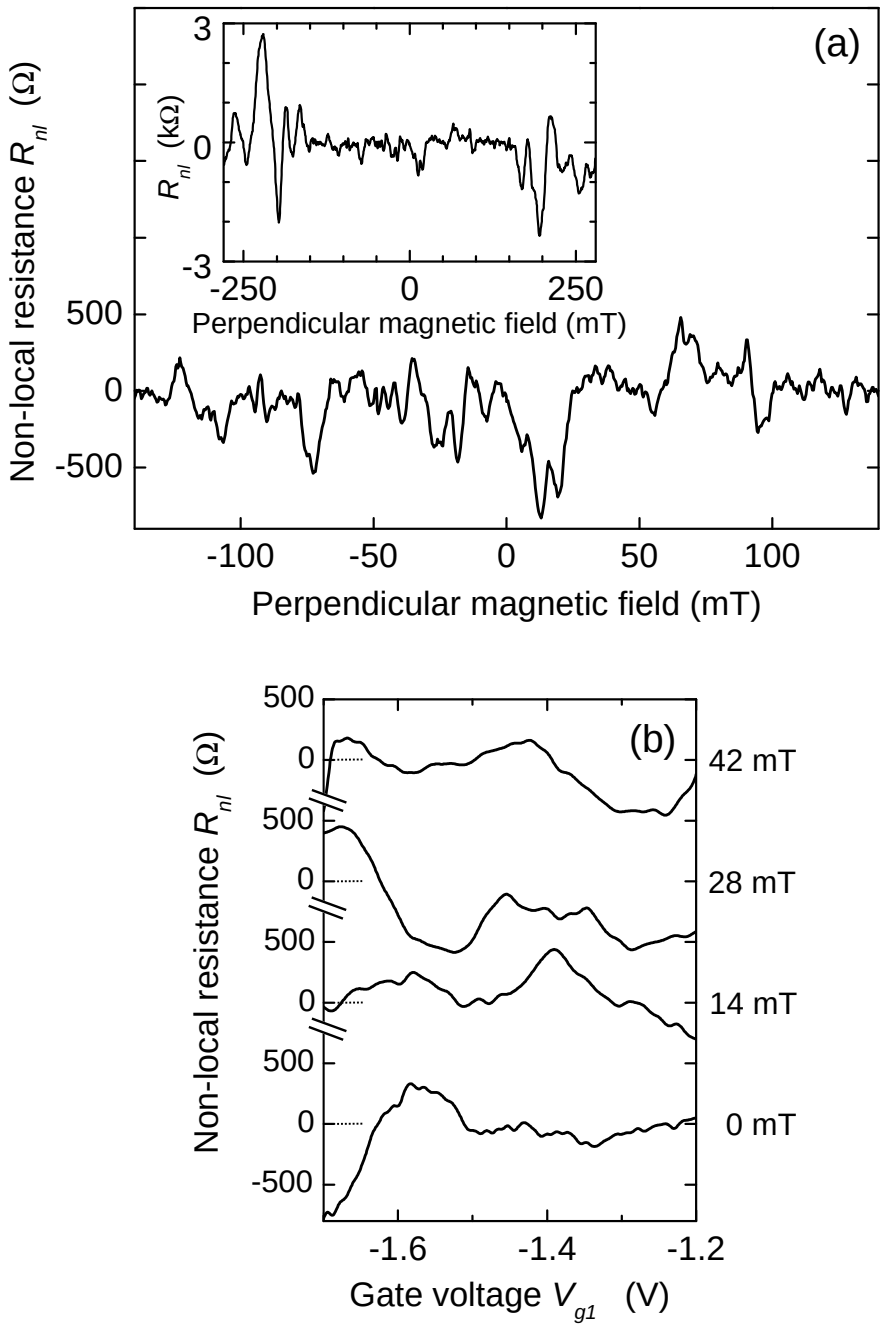

Figure 6.4: **(a)** The non-local resistance R_{nl} as a function of magnetic field. The magnetic field is given on the scale of the perpendicular component of the total applied field. For this measurement all four QPCs are defined to have a conductance of $2e^2/h$. The inset presents the same data for a wider range of the magnetic field, showing the onset of electron focusing effects for perpendicular fields larger than ± 140 mT. The curves in **(b)** show the non-local resistance as a function of the voltage applied to gate $g1$ at different values of the perpendicular magnetic field. The conductance of the QPC formed by $g5$ and $g6$ (defining the V_- probe) is kept at $2e^2/h$. For further experimental parameters see Fig. 6.2.

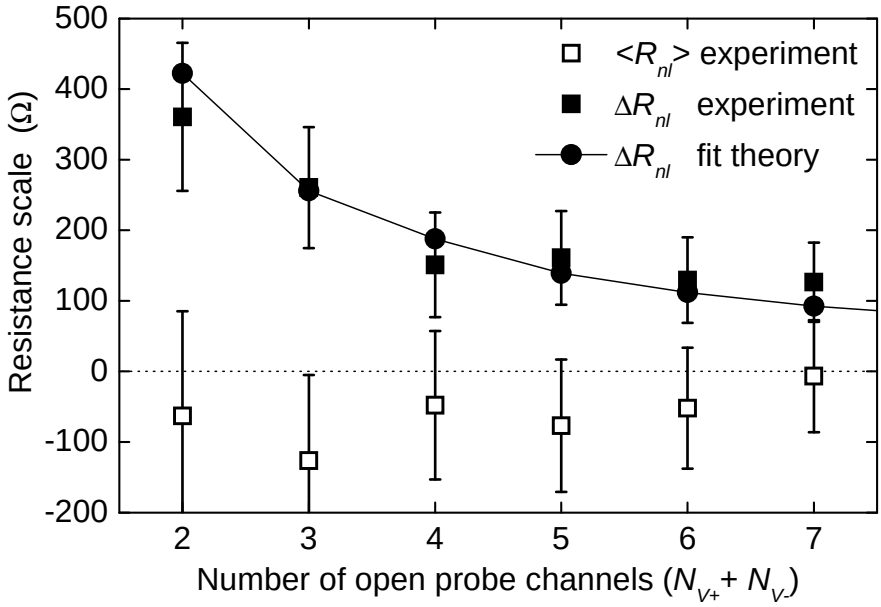

Figure 6.5: Dependence of the mean $\langle R_{nl} \rangle$ and rms standard deviation ΔR_{nl} of fluctuations in the measured non-local resistance R_{nl}, as a function of the total number open of channels in the voltage probes $N_{V+} + N_{V-}$ (squared dots). The statistics are from sets of data as in Fig. 6.2, but with time-reversal symmetry broken by weak magnetic fields ($\beta = 2$). The round dots with solid line present a fit of the theoretical model that describes the values of ΔR_{nl} (see text for details).

amplitude of the fluctuations decreases when the voltage probes get more open channels. For a more quantitative analysis of this observation, we determined the mean $\langle R_{nl} \rangle$ and root-mean-square (rms) standard deviation ΔR_{nl} of the non-local resistance for traces recorded at a fixed number of channels in the voltage probes. This can be obtained by following R_{nl} along lines with constant $N_{V+} + N_{V-}$. The theory in the next section shows that, on such a line, ΔR_{nl} should also show a weak dependence on N_{V+} - N_{V-}. However, we do not have sufficient data to study this, and simply average along lines with constant $N_{V+} + N_{V-}$. The results of this analysis are presented in Fig. 6.5. The large error bars for $\langle R_{nl} \rangle$ and ΔR_{nl} in Fig. 6.5 are due to the fact that we could only record a finite number of independent data sets with fluctuations in R_{nl} (see Ref. [40] for further details).

The results in Fig. 6.5 confirm that $\langle R_{nl} \rangle$ is very close to zero, for all values of $N_{V+} + N_{V-}$. More interestingly, ΔR_{nl} smoothly decreases as a function $N_{V+} + N_{V-}$, demonstrating directly the dephasing influence of the voltage probes for

the electrons in the quantum dot. The typical fluctuation amplitude approaches zero when the dot becomes fully open (very strong coupling to a reservoir). For a quantitative evaluation of this observation, we will first present a theoretical model in the next Section.

6.5 Theoretical analysis and discussion

For our theoretical modeling we consider a ballistic chaotic cavity connected to four reservoirs through quantum point contacts. A net current I flows between two of the contacts (from I_+ to I_-), while there is no net current flowing into two contacts used as voltage probes (contacts V_+ and V_-). We use the Landauer-Büttiker formalism to derive the relations between the current I and the voltages of the four contacts [21],

$$I = \frac{1}{2}\left(\frac{2e^2}{h}\right)[((N_1 - T_{11}) + (N_2 - T_{22}) + T_{12} + T_{21})\,\frac{V_{bias}}{2} + (T_{23} - T_{13})V_3 + (T_{24} - T_{14})V_4], \tag{6.1a}$$

$$V_3 = \frac{V_{bias}}{2}\frac{(N_4 - T_{44})(T_{31} - T_{32}) + T_{34}(T_{41} - T_{42})}{(N_3 - T_{33})(N_4 - T_{44}) - T_{34}T_{43}}, \tag{6.1b}$$

$$V_4 = \frac{V_{bias}}{2}\frac{(N_3 - T_{33})(T_{41} - T_{42}) + T_{43}(T_{31} - T_{32})}{(N_3 - T_{33})(N_4 - T_{44}) - T_{34}T_{43}}, \tag{6.1c}$$

where we used (for concise labeling) notation according to

$$\begin{aligned} I_+ &\leftrightarrow 1, \\ I_- &\leftrightarrow 2, \\ V_+ &\leftrightarrow 3, \\ V_- &\leftrightarrow 4. \end{aligned}$$

Here the T_{ij} are the transmission probabilities from contact i to j, while the N_i are the number of open channels in contact i. The voltages V_i are all defined with respect to a ground [41] which is defined such that $V_1 = +V_{bias}/2$ and $V_2 = -V_{bias}/2$, where $V_{bias} = V_1 - V_2$ is the voltage across the dot in the current path that is consistent with a bias current I. The measured voltage V in the experiments corresponds to the quantity $V = V_3 - V_4$, and the non-local resistance is then

$$R_{nl} = \frac{V_3 - V_4}{I}. \tag{6.2}$$

We obtain the mean and root-mean-square (rms) of the R_{nl} by generating a set of random scattering matrices with the kicked rotator [23, 24]. The kicked rotator gives a stroboscopic description of the dynamics in the quantum dot, which is a good approximation of the real dynamics for time scales larger then the time of flight across the dot. The particular implementation we used is described in detail in Ref. [42]. In a certain parameter range, this model gives results which are equivalent to random matrix theory [3]. In our simulations we use parameters in this range, the details of which can be found in Ref. [42].

Figure 6.6 presents the results from these numerical simulations. We focus on analysis of the fluctuations in R_{nl}, since the mean values of R_{nl} simply always gave zero, in agreement with the experimental results [21]. Figure 6.6a shows the dependence of the fluctuations in R_{nl} on the total number of open channels in the voltage probes $N_{V+} + N_{V-}$, for systems with time-reversal symmetry ($\beta = 1$) and broken time-reversal symmetry ($\beta = 2$). The results in Fig. 6.6b show that the fluctuations in R_{nl} have (besides a strong dependence on $N_{V+} + N_{V-}$ as in Fig. 6.6a) a weak dependence on the difference N_{V+} - N_{V-} (presented only for the case $\beta = 2$). This is not further studied in detail, and the results in Fig. 6.6a present values that are averaged over all the possible combinations N_{V+} - N_{V-}, as in the analysis of the experimental results.

Qualitatively, the theoretical results of Fig. 6.6a agree very well with the experimental results of Fig. 6.5. However, while the model system gives non-local resistance R_{nl} values that fluctuate with an rms value of a few kΩ, the experimental values ($\beta = 2$) are only of order 200 Ω. The numerical and experimental values differ by a factor of about 20, as illustrated by the fit in Fig. 6.5: Fitting the theoretical data points of Fig. 6.6 on the experimental values, using a simple pre-factor that scales the theoretical values as fitting parameter, gives $0.05 \approx \frac{1}{20}$ for this pre-factor.

The discrepancy between the numerical and the experimental results is most likely due to orbital dephasing for electrons inside the quantum dot. Moreover, such dephasing is possibly consistent with the simple scaling that was needed to obtain agreement between theory and experiment. Theory for two-terminal quantum dots gives that the influence of dephasing on the amplitude of conductance fluctuations is that it scales the amplitude down by a factor $(1 + \tau_d/\tau_\phi)$, where τ_d is the mean dwell time in the dot and τ_ϕ is the dephasing time [43, 38]. Assuming a similar approach for our system, then gives $(1 + \tau_d/\tau_\phi) \approx 20$. However, it is at this stage not clear whether this theory work for two-terminal dots can be applied to our system, and we can also not rule out that the effective

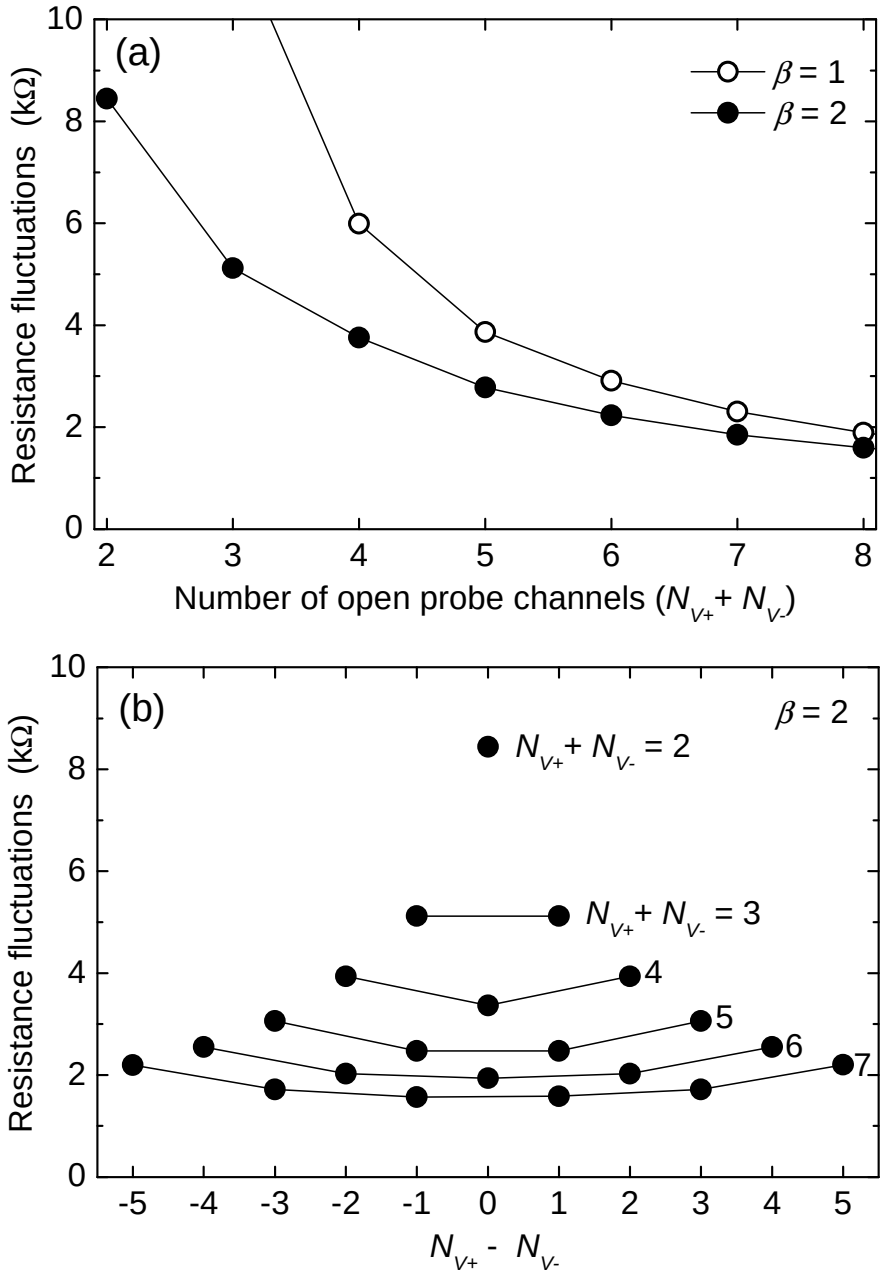

Figure 6.6: **(a)** Theoretical rms values of fluctuations in the non-local resistance (ΔR_{nl}), as a function of the total number open of channels in the voltage probes $N_{V+} + N_{V-}$. The two curves present results for a system with ($\beta = 1$) and without ($\beta = 2$) time-reversal symmetry. The QPCs for the current path were assumed to have a conductance of $2e^2/h$. The data is obtained from a Landauer-Büttiker description of the quantum dot system and numerical simulations based on random matrix theory. **(b)** Theoretical rms values of fluctuations in R_{nl}, as a function of the difference in number open of channels in the two voltage probes, $N_{V+} - N_{V-}$, at fixed values of $N_{V+} + N_{V-}$. The data in a) presents ΔR_{nl} values for $N_{V+} + N_{V-}$, that have been averaged over all possible combinations of $N_{V+} - N_{V-}$.

electron temperature of about 400 mK plays a role in reducing the fluctuation amplitude. Nevertheless, it is interesting to compare the factor $(1 + \tau_d/\tau_\phi)$ that we need to use here to independently determined values for τ_d and τ_ϕ.

For the dwell time we use the expression[32] $\tau_d = h/N_\Sigma\Delta_m$, where N_Σ the total number of open modes in the contacts to the dot, and $\Delta_m = 2\pi\hbar^2/m^*A_{dot}$ the mean spacing between energy levels in the dot. This gives $\tau_d \approx 470$ ps for our system tuned to have all four QPCs at $N = 1$. The most reliable method for estimating the dephasing time τ_ϕ is based on a measurement of the depth of the weak localization dip in the two-terminal conductance [30, 5]. In such measurements on our system (with all four QPCs tuned to $N = 1$) we observed a weak localization dip of $\delta g = 0.045 \pm 0.01(e^2/h)$ in a background of $0.88(e^2/h)$ (the large error bar is again due to the fact that we could only average over a few independent fluctuations in the two-terminal conductance). Following Refs. [30, 5], we derive the dephasing time using $\delta g = (e^2/h) \cdot N/(2N + N_\phi)$ and $\tau_\phi = h/N_\phi\Delta_m$. Here N_ϕ is the number of open modes to a fictitious voltage probe that is responsible for dephasing in the dot, and N is now the number of modes per lead for a two-terminal dot, so we set it to $N = 2$ for our system with four QPCs tuned to $N = 1$. This yields $N_\phi \approx 40$ and $\tau_\phi = 46 \pm 12$ ps for our system at ~ 400 mK, in reasonable agreement with earlier two-terminal studies on similar systems [30, 5, 31].

The independently determined values for τ_d and τ_ϕ give for the factor $(1 + \tau_d/\tau_\phi) \approx 11$, which differs only by a factor ~ 2 from the value 20 that we obtained from the scaling. This supports the assumption that the reduction in the fluctuation amplitude ΔR_{nl} is due to orbital dephasing inside the dot. However, the above analysis is only valid for all QPCs of the dot tuned to $N = 1$. While we can apply a single scaling factor for all values of $N_{V+} + N_{V-}$ in Fig. 6.5, τ_d decreases in fact significantly with increasing $N_{V+} + N_{V-}$. Moreover, it is tempting to consider that the reduction in ΔR_{nl} can be understood by assuming that dephasing in the dot increases the value of $N_{V+} + N_{V-}$ to an effective value of $N_{V+} + N_{V-} + N_\phi$. However, this is clearly not in agreement with the observed drop in ΔR_{nl} over the interval $N_{V+} + N_{V-}$ in Fig. 6.5. This indicates that new theoretical work specific for the role of dephasing for a four-terminal dot is needed for a complete understanding of the data in Fig. 6.5.

6.6 Conclusions

We investigated quantum fluctuations in electron transport with a ballistic, chaotic quantum dot that was strongly coupled to four reservoirs via quantum point contacts. The four-terminal geometry allowed for studying fluctuations in the non-local resistance. We used the dependence of the non-local resistance fluctuations on bias voltage, gate voltage and magnetic field to show that these are the equivalent of universal conductance fluctuations in two-terminal systems, and we showed that with a four-terminal system these fluctuations can be studied without being hindered by Coulomb-blockade and weak-localization effects. Furthermore, the four-terminal geometry was used to demonstrate directly that the amplitude of fluctuations in electron transport is reduced when the coupling between a quantum dot system and voltage probes is enhanced. Here, we obtain good qualitative agreement with a model based on Landauer-Büttiker formalism and random matrix theory, but a quantitative evaluation indicates that there is an intrinsic orbital dephasing mechanism that reduces the amplitude of the non-local resistance fluctuations. Our results are of importance for further work with four-terminal quantum dots on dephasing and electron-spin dynamics in such systems, where the electron-transport signals of interest will always have fluctuations of the type that is reported here.

We thank Dominik Zumbühl and Carlo Beenakker for discussions, and the Dutch Foundation for Fundamental Research on Matter (FOM) for financial support.

References

[1] B. L. Al'tshuler and P. A. Lee, Physics Today, Issue of December 1988, p. 36.

[2] C. W. J. Beenakker and H. van Houten, Sol. State Phys. **44**, 1 (1991).

[3] C. W. J. Beenakker, Rev. Mod. Phys. **69**, 731 (1997).

[4] Y. Imry, *Introduction to Mesoscopic Physics*, Oxford University Press, Oxford, 2002.

[5] A. G. Huibers, M. Switkes, and C. M. Marcus, Phys. Rev. Lett. **81**, 200 (1998).

[6] A. G. Huibers *et al.*, Phys. Rev. Lett. **81**, 1917 (1998).

[7] E. R. P. Alves and C. H. Lewenkopf, Phys. Rev. Lett. **88**, 256805 (2002).

[8] D. M. Zumbühl *et al.*, Phys. Rev. B **72**, 081305 (2005).

[9] M. Büttiker, Phys. Rev. Lett. **57**, 1761 (1986).

[10] A. Benoit *et al.*, Phys. Rev. Lett. **58**, 2343 (1987).

[11] W. J. Skocpol *et al.*, Phys. Rev. Lett. **58**, 2347 (1987).

[12] H. Haucke *et al.*, Phys. Rev. B **41**, 12454 (1990).

[13] M. Büttiker, Phys. Rev. B **40**, 3409 (1989).

[14] H. U. Baranger and P. A. Mello, Phys. Rev. Lett. **73**, 142 (1994).

[15] R. M. Potok *et al.*, Phys. Rev. Lett. **89**, 266602 (2002).

[16] A. Venkatesan *et al.*, 2007 March Meeting Bulletin of the American Physical Society (unpublished), Abstract H12.00012.

[17] F. J. Jedema, A. T. Filip, and B.J. van Wees, Nature **410**, 345 (2001).

[18] J. A. Folk *et al.*, Science **299**, 679 (2003).

[19] D. M. Zumbühl *et al.*, 2001 March Meeting Bulletin of the American Physical Society (unpublished), Abstract C25.006.

[20] C. W. J. Beenakker, Phys. Rev. B **73**, 201304 (2006).

[21] J. H. Bardarson, I. Adagideli, and P. Jacquod, Phys. Rev. Lett. **98**, 196601 (2007).

[22] R. Landauer, IBM J. Res. Dev. **1**, 223 (1957).

[23] F. M. Izrailev, Phys. Rep. **196**, 299 (1990).

[24] Y.V. Fyodorov and H.-J. Sommers, JETP Lett. **72**, 422 (2000).

[25] B. J van Wees *et al.*, Phys. Rev. Lett. **60**, 848 (1988).

[26] D. A. Wharam *et al.*, J. Phys. C: Solid State Phys. **21**, L209 (1988).

[27] P. Debray *et al.*, Phys. Rev. Lett. **63**, 2264 (1989).

[28] J. A. Folk *et al.*, Phys. Rev. Lett. **86**, 2102 (2001).

[29] D. M. Zumbühl *et al.*, Phys. Rev. B **69**, 121305 (2004).

[30] C. M. Marcus *et al.*, Chaos Solitons Fractals **8**, 1261 (1997); cond-mat/9703038.

[31] A. G. Huibers *et al.*, Phys. Rev. Lett. **83**, 5090 (1999).

[32] C. M. Marcus *et al.*, Phys. Rev. B **48**, 2460 (1993).

[33] I. H. Chan *et al.*, Phys. Rev. Lett. **74**, 3876 (1995).

[34] C. W. J. Beenakker and H. van Houten, Phys. Rev. B **37**, 6544 (1988).

[35] H. van Houten *et al.*, Phys. Rev. B **39**, 8556 (1989).

[36] K. Kobayashi *et al.*, J. Phys. Soc. Japan, **71**, 2094 (2002).

[37] G. Seelig *et al.*, Phys. Rev. B **68**, 161310 (2003).

[38] P. W. Brouwer and C. W. J. Beenakker, Phys. Rev. B **51**, 7739 (1995).

[39] P. W. Brouwer and C. W. J. Beenakker, Phys. Rev. B **55**, 4695 (1997).

[40] Analysis of the error bars is in particular relevant for low values of $N_{V+} + N_{V-}$, for which we could only obtain a few independent fluctuations. We used that we had the largest amount of data for traces with $N_{V+} + N_{V-} = 7$. Here we had sufficient data to estimate $\Delta R_{nl} = 126 \pm 56\ \Omega$. For traces with lower $N_{V+} + N_{V-}$, we used that the number of independent fluctuations n_f along a trace with constant $N_{V+} + N_{V-}$ is simply proportional to $N_{V+} + N_{V-}$ for data sets as in Fig. 6.2, since it is proportional to the trace length through the data set. We assume a gaussian distribution for the fluctuations. Then, we used that for a finite number n_f of independent fluctuations, the error bar for $\langle R_{nl} \rangle$ depends on n_f as $1/\sqrt{n_f}$, and for ΔR_{nl} (on the same scale) as $1/\sqrt{2n_f}$.

[41] Note that this definition for ground differs from the grounding used the in the experiment. However, since in our experiments the values of the gate voltages were much larger than the values of V_{bias}, our theoretical model is a valid description of the experiment.

[42] J. H. Bardarson, J. Tworzydło, and C. W. J. Beenakker, Phys. Rev. B **72**, 235305 (2005).

[43] H. U. Baranger and P. A. Mello, Phys. Rev. B **51**, 4703 (1995).